ELSEVIER

Journal of Photochemistry and Photobiology A: Chemistry 122 (1999) 199–204

Journal of Photochemistry and Photobiology A:Chemistry

Kinetic modelling of the photochromism and photodegradation of a spiro[indoline-naphthoxazine]

V. Pimienta[a], C. Frouté[a], M.H. Deniel[a], D. Lavabre[a], R. Guglielmetti[b], J.C. Micheau[a,*]

[a]*IMRCP, UMR CNRS 5623, Université Paul Sabatier, 118 Route de Narbonne, F-31062, Toulouse Cédex, France*

[b]*LCMOM, ESA CNRS 6411, Université de Ia Méditerranée, Faculté des Sciences de Luminy, Case 901, F-13288, Marseille Cédex, France*

Received 30 November 1998; accepted 25 January 1999

Abstract

The photochromism of the 1,3,3-trimethylspiro[indoline-naphthoxazine] **A** has been studied under continuous monochromatic irradiation (313 and 365 nm) in liquid toluene solution at 278 K. The values of the main photochromic parameters (quantum yields and absorption coefficients) have been determined by kinetic modelling of absorbance (Abs) versus time curves recorded under continuous irradiation. We showed that the quantum yields of both photocoloration and reversible photochemical bleaching were wavelength-dependent. Under 365 nm irradiation, photodegradation processes that are not sensitive to the presence of oxygen were observed. The degradation occurs either from the direct irradiation of the closed spiro form **A** or from the thermal decomposition of the open photomerocyanine form **B**. Under our experimental conditions, photochemical decomposition of the open photomerocyanine form **B** was negligible.

Keywords: Photochromism; Kinetic modelling; Spironaphthoxazine; Photomerocyanine; Photodegradation

1. Introduction

Photochromism is a photoinduced reversible phenomenon (i.e. the transformation of a photosensitive substrate into an isomer exhibiting a different absorption spectrum in the visible region). Photochromic compounds are of interest for practical applications like variable optical filters. Development of such applications requires (besides the elaboration of new compounds), a detailed understanding of the mechanisms involved, including those of the photodegradation processes.

Spiro-compounds are the most well-known organic photochromes. Among them, spiro-[indoline-naphthoxazines] (spironaphthoxazines) comprise two heterocyclic moieties linked by a tetrahedral spiro-carbon which prevents them from being conjugated. 1,3,3-trimethylspiro[indoline-naphthoxazine] **A** that corresponds to the unsubstituted basic skeleton has been submitted to extensive investigations [1]. Under UV irradiation, the C_{spiro}–O bond breaks, facilitating the formation of the quasi-planar open form **B** (photomerocyanine). This bond cleavage is believed to occur in the sub-picosecond time-scale leading to a fast equilibrated mixture where the transoid–transoid–cisoid conformer (TTC) predominates [2–5] (Scheme 1). For a long time-scale, this mixture behaves as a single species. Photomerocyanine **B** shows a characteristic absorption band in the visible region due to the extended conjugation of π electrons. It has been suggested that the open form **B** is able to undergo ring closure to the initial spiro-compound either thermally or photochemically [6,7].

The literature related to the determination of quantum yields (Φ) or molar extinction coefficients of the open form **B** (ε_B) of the spironaphthoxazine **A** is rather contradictory and incomplete. As a possible explanation, it must be pointed out that these determinations are not a trivial problem because the concentration of **B** needs to be known

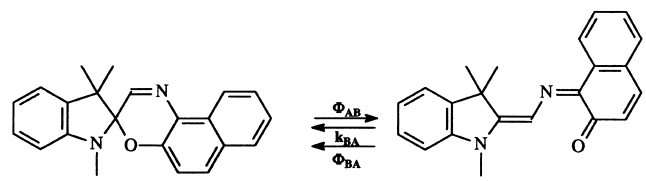

A **B**

uncolored closed form **quinoïdal TTC colored open form**

Scheme 1.

*Corresponding author.

1010-6030/99/$ – see front matter
PII: S1010-6030(99)00023-4

with precision. Flash photolytic techniques [8] based on absorption measurements after excitation or 'colourability' experiments [9] are difficult to interpret without any external assumption as they always provide the product '$\Phi.\varepsilon_B$' and never each individual term. To avoid this difficulty, it is often assumed that low temperature or high intensity experiments lead to a 'nearly completely converted' system from which the molar absorption coefficient of the photomerocyanine **B** could be readily obtained. However, this is not always true because photobleaching can also occur. It is generally recognised that thermal bleaching after photocoloration (i.e. thermal ring closure of **B** to the initial spironaphthoxazine **A**) obeys first-order kinetics [10–13] and that this reaction is accelerated by the presence of traces of acid [14]. Photodegradation processes have also been investigated [15–18]. Results show that photo-oxidation plays an important role but other competitive non-oxidative processes also occur [19]. It then appears that the photochemistry of the spironaphthoxazine involves several simultaneous photochemical and thermal processes and that the determination of quantum yields and rate constants of each individual process is not an easy task. From this point of view, continuous irradiation methods and kinetic analysis [20–24] deserve a special mention because, in simple cases, the estimation of some photochromic parameters is possible. In this paper, it is shown that kinetic modelling of absorbance (Abs) versus time curves recorded under continuous monochromatic irradiation allows to obtain quantitative information related to the photochromism and the photodegradation of the spironaphthoxazine **A**.

2. Photochromism of the spironaphthoxazine

2.1. Kinetic modelling

In this section, we will focus on the photochromic process, ignoring photodegradation. For short continuous irradiation time (<40 s), photodegradation can be neglected as the absorbance stabilises at a photosteady state. The photochromism of the spironaphthoxazine **A** in toluene solution can be described by the kinetic Scheme 2, which involves three processes: the photoisomerisation of the closed form **A** to the photomerocyanine **B** and re-isomerisation from **B** to **A**, twice, one thermal and one photochemical.

Two experiments were carried out using two irradiation wavelengths ($\lambda' = 365$ nm and $\lambda'' = 313$ nm). For each run, the evolution of the absorbance under continuous monochromatic irradiation was monitored at two wavelengths: the irradiation wavelength λ' or λ'' and the λ_{max} of the photomerocyanine **B** (592 nm) (see Fig. 1).

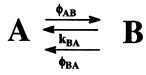

Scheme 2.

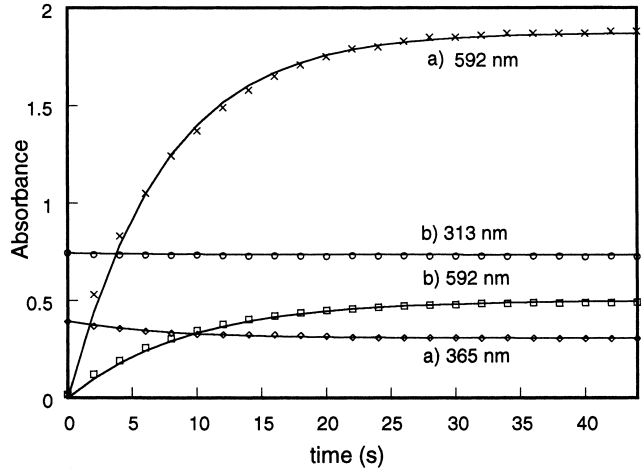

Fig. 1. Plot of the absorbance at 592 nm and at the irradiation wavelength of a non-degassed toluene solution of spironaphthoxazine **A** under continuous irradiation at two monochromatic wavelengths (a) 365 nm and (b) 313 nm. Experimental parameters were $[A_0] = 1.02 \times 10^{-4}$ mol l^{-1}, $\varepsilon_A^{313} = 6690$, $\varepsilon_A^{365} = 3660$ l mol^{-1} cm^{-1}, $\varepsilon_A^{592} = 0$, (a) $I_0^{365} = 2.2 \times 10^{-5}$ mol l^{-1} s^{-1} and $k_{BA} = 6.2 \times 10^{-2}$ s^{-1}, (b) $I_0^{313} = 0.6 \times 10^{-5}$ mol l^{-1} s^{-1} and $k_{BA} = 7.5 \times 10^{-2}$ s^{-1} ($T = 278$ K). Values of the fitted parameters are listed in Table 1.

The four kinetic curves were fitted simultaneously using the kinetic model shown in Scheme 2 (see Experimental section for the corresponding rate equations). For these calculations, all the parameters that were experimentally accessible were fixed. The initial concentration of the spironaphthoxazine **A** ($[A]_0$) and its UV–Vis spectrum were determined (ε_A^λ). The thermal ring closure rate constant (k_{BA}) was measured at the end of each run. We checked that the monochromatic photon fluxes at the irradiation wavelengths ($I_0^{\lambda'}$ and $I_0^{\lambda''}$) remained within ±5% between the start and the end of each experiment. Fitted parameters are the values of the quantum yields of photocolouration (Φ_{AB}) and photobleaching (Φ_{BA}) together with the molar extinction coefficients of the open form **B** (ε_B^{313}, ε_B^{365} and ε_B^{592}). During the parameters optimisation procedure, we found that neglecting the photobleaching process (i.e. taking $\Phi_{BA} = 0$) failed to give a satisfactory fit. Moreover, to reproduce perfectly the kinetic curves obtained using the two different irradiation wavelengths, we had to introduce a wavelength dependence for the photocoloration and photobleaching quantum yields. Values of the parameters that give satisfactory fitting are listed in Table 1. The absolute errors given in this table take into account that satisfactory curve fitting can be obtained with a slightly different set of fitted parameters. Extreme values have been considered in each case.

Table 1
Parameter values from the curve fitting on Fig. 1

	313 nm	365 nm	592 nm
Φ_{AB}	0.3 ± 0.05	0.5 ± 0.1	–
Φ_{BA}	1.4 ± 0.2	0.3 ± 0.2	–
ε_B	5400 ± 400	1500 ± 400	40 000 ± 7000

2.2. Quantum yield of photobleaching Φ_{BA}

No satisfactory fitting can be obtained without taking this process into account. This result is interesting as this is for the first time that approximate values of the photobleaching quantum yield Φ_{BA} have been estimated for the spironaphthoxazine **A**. Our results also show that visible irradiation is not required for photochemical ring closure and that photomerocyanine **B** exhibits photoreactive absorption bands in the same region as the closed form **A**. In these conditions, measurement techniques based on the assumption that at low temperature or under high photon flux, the closed form **A** could be nearly completely converted into the open form **B** (i.e. $[B] = 100\%\ [A]_0$) should be viewed with caution since due to the photobleaching process, the conversion rate may be reduced to an unknown extent.

2.3. Wavelength dependence of Φ_{AB} and Φ_{BA}

Values of the same order of magnitude as those reported in the literature [25] were found for Φ_{AB}. Moreover, our kinetic analysis shows that in toluene solution at 278 K, the quantum yield of photocoloration Φ_{AB} is wavelength-dependent, being higher for longer wavelength. Such a property has been described by Kholmanski et al. [26] in EtOH at 243 K, who reported values similar to ours ($\Phi_{AB} = 0.22$ at 313 nm and 0.41 at 365 nm). In order to interpret this wavelength effect, it has been suggested that 365 nm irradiation light which is absorbed by the oxazine moiety is expected to be more efficient in breaking the C_{spiro}–O bond than 313 nm light which is absorbed by the indoline moiety. The photobleaching quantum yield is also wavelength-dependent. Φ_{BA} at 365 nm was estimated to be around 0.3 ± 0.2, this value being of the same order of magnitude as the photocoloration quantum yield Φ_{AB} at the same irradiation wavelength. Φ_{BA} at 313 nm was even higher with a fitting value around 1.4 ± 0.2. This value exceeding unity may perhaps be accounted for by experimental errors or by a defect in the model. However, another interpretation could be that the formation of 313 nm light induced protonated photomerocyanine ($\mathbf{BH}^+$). It is known that this species is able to catalyse the thermal ring closure, thus providing an extra amount of the rate of reisomerisation from **B** to **A**. Using two irradiation wavelengths, Bohne et al. [6,7] have suggested that in a non-polar solvent, photomerocyanine **B** regenerates the starting material by visible light irradiation. However, no value of Φ_{BA} has been given. Other authors recognize the existence of a photobleaching process [27,28], while others just neglect it [29] or simply do not mention it.

2.4. Molar extinction coefficient of the photomerocyanine **B** (ε_B^λ)

From the whole spectrum of the reacting medium under continuous irradiation and using calculated photoconversion rate, the spectrum (ε, L mol^{-1} cm^{-1}) of the photomerocyanine **B** can be obtained (see Fig. 2).

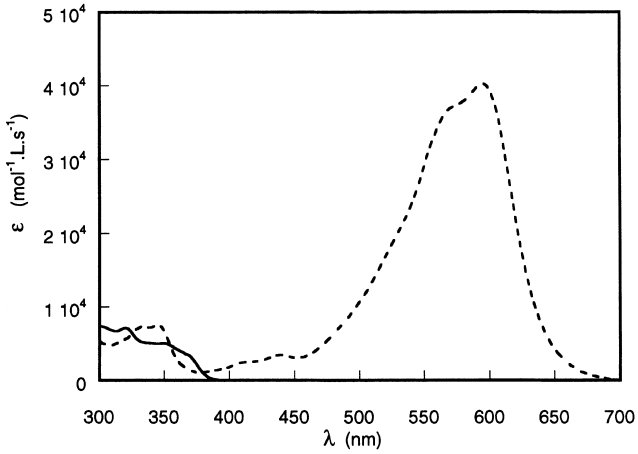

Fig. 2. Dashed line: calculated UV–Vis spectrum (ε, L mol^{-1} cm^{-1}) of the photomerocyanine **B**. Continuous line: measured spectrum of the spironaphthoxazine **A** (note the presence of several bands and shoulders on both spectra in the UV region). The solvent is toluene at 278 K.

Our numerical calculation leads to $\varepsilon_B^{592} = 40\,000 \pm 7000$ l mol^{-1} cm^{-1} in toluene at 278 K. This value is comparable to literature data: Wilkinson et al. [29] give 31 000 in the same solvent and Favaro et al. [30], 38 000 in methylcyclohexane at room temperature. Values from 52 000–81 000 (L mol^{-1} cm^{-1}) are given in polar solvent [31,32]. We have calculated the spectrum of the photomerocyanine **B** even in the wavelength region where **A** is involved in absorption. The spectrum of **B** clearly exhibits several absorption bands in this region.

3. Photodegradation of the spironaphthoxazine

3.1. Kinetic modelling

For longer irradiation periods, an irreversible degradation of the photochromic properties occurred (see Fig. 3). This effect is known as photodegradation simply because it is caused by light irradiation of the photochromic compound without making any mechanistic assumptions. In order to avoid parasitic phenomena in the irradiation of toluene, we chose to conduct the photodegradation experiments under 365 nm monochromatic irradiation. At this wavelength, toluene does not carry out absorption. In contrast to the experiments carried out at 313 nm (where oxygen accelerates photodegradation), our experiments at 365 nm showed no difference between oxygen and argon bubbled photodegradation kinetics. This result may appear surprising as most of the photodegradation effects stem from photooxidation i.e. in the presence of oxygen [33]. However, it should be pointed out that there is an important difference between our experiment and the conventional photooxidation studies. In order to simulate daylight, conventional photooxidation

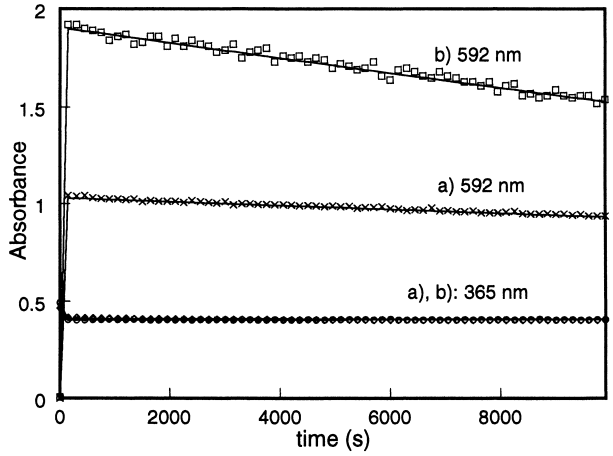

Fig. 3. Plot of the absorbance recorded at 592 and 365 nm (irradiation wavelength) of an argon bubbled toluene solution of spironaphthoxazine **A** (1.3×10^{-4} mol l^{-1}) under continuous irradiation at two successive incident photon fluxes (a) $I_0 = 0.66 \times 10^{-5}$ and (b) $I_0 = 1.43 \times 10^{-5}$ mol l^{-1} s^{-1} ($T = 278$ K). Oxygen bubbled experiments produced similar results.

studies are often carried out using high pressure polychromatic Xe or Hg lamps, allowing direct irradiation of the highly absorbing charge transfer visible band of the photomerocyanine **B**. Lower energy excited states of **B** are produced, and in the presence of oxygen, they lead to photooxidation processes. Under 365 nm monochromatic irradiation, such photooxidation is unlikely to take place and photodegradation will thus not be oxygen-sensitive. In order to construct a photodegradation model (see Scheme 3), we therefore added three irreversible degradation processes, two from **B** (one thermal and one photochemical) and one photochemical degradation from **A** to the previous photochromic Scheme 2. The corresponding photodegradation products were **C**, **D** and **E**, respectively. Their chemical structures have not been specified. Corresponding rate equations can be found in the Experimental section.

A more than 200-fold longer duration of irradiation than that used for the previous experiment was employed at two different values of light intensity. Variation in the monochromatic light irradiation photon flux could distinguish between a thermal degradation from **B** (its rate law would be independent of I_0) or a photochemical one (its rate law would be dependent on I_0).

3.2. Parameters of photodegradation

These curves were simultaneously fitted using the kinetic Scheme 3 model. All the parameters obtained from the previous fitting in Fig. 1 were set to their optimised values.

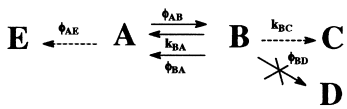

Scheme 3.

Only the parameters related to the formation of **C**, **D** and **E** were fitted. During this calculation, it was impossible to obtain satisfactory simultaneous curve fitting if direct photochemical decomposition of **B** was considered (i.e. if Φ_{BD} was taken $\neq 0$). It can be concluded that degradation under 365 nm irradiation does not originate from the photochemical excitation of the open form **B**. However, using these experimental curves, our kinetic modelling technique was not able to discriminate between the two other irreversible processes that were considered, namely a direct photochemical decomposition of **A** or a thermal decomposition of **B**. If we consider only the photochemical decomposition of **A**, the quantum yield would be $\Phi_{AE} = 5 \times 10^{-4}$, while on the other hand, if there was only thermal degradation from **B**, the rate constant k_{BC} would be 7×10^{-5} s^{-1}. This last hypothesis is in line with literature data [19] reporting that a small proportion of ground state photomerocyanine **B** does not undergo ring closure to **A** but decomposes itself or reacts with the solvent.

Using the extent of degradation from the model, we calculated the UV spectrum of the whole set of photodegradation products. The same spectrum was obtained with oxygen and argon bubbling. It is thus likely that the set of these photodegradation products are of non-oxidative origin. A possible primary reaction mechanism is assumed to be a cleavage of C_{spiro}–C in **B**, leading to naphth[l,2-d]oxazole **1**

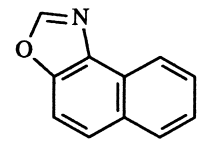

1

whose UV spectrum ($\lambda^{max} = 321$ nm, $\varepsilon^{321} = 3300$ l mol^{-1} cm^{-1} in toluene solution) is not incompatible with the extracted UV spectrum of the whole set of photodegradation products ($\lambda^{max} = 321$ nm, $\varepsilon^{321} = 4500$ l mol^{-1} cm^{-1}). Other compounds derived from the interaction of **B**, with toluene acting as an hydrogen-donating solvent or from the radical reaction of the indoline moiety are likely. However, their spectra cannot be extracted with sufficient accuracy to enable comparison with authentic samples.

4. Conclusions

Our study shows that pertinent information can be obtained from the kinetic modelling of Abs versus time curves recorded under continuous monochromatic irradiation of photochromic spironaphthoxazine **A** in toluene solution at 278 K. Φ_{AB} is wavelength-dependent, being higher for longer irradiation wavelength. Photobleaching also occurs at the same irradiation wavelength as photocolouration, the values of the photobleaching quantum yield being of the same order of magnitude or even higher than that of photocolouration. Under 365 nm continuous irradia-

tion, there is a photodegradation process which is not oxygen-dependent. Kinetic analysis shows that, at this wavelength, photochemical degradation from the photomerocyanine **B** is negligible. Degradation occurs either from direct irradiation of the closed form **A** or more likely from thermal decomposition of the open form **B**.

5. Experimental

5.1. Kinetic runs

Spironaphthoxazine **A** was supplied by Enichem Synthesis and used without further purification. The solvent was spectroscopic grade toluene. The irradiation was derived from a 200 W high-pressure Hg lamp equipped with shutter, interference filters and fibre optic light conductor. The 2.1 ml reactor was a quartz cylinder closed with a Teflon bung allowing gas bubbling. The contents were stirred continuously with a magnetic bar driven by a speed controlled stepper motor. The whole set-up was enclosed in a thermostatic copper block at 278 K and placed inside the sample chamber of a HP8451 diode array spectrophotometer. Monochromatic light intensity was determined directly in the reactor using an aqueous solution of 5×10^{-4} mol l^{-1} of potassium ferrioxalate at pH 1 [34]. Measurement of the extent of photoreduction of Fe^{III} was performed by UV–Vis spectrophotometry without using 1,10-phenanthroline complexation. Spectroscopic parameters and quantum yields that were used are: $\lambda' = 313$ nm, $\Phi = 1.24$, $\varepsilon_{FeIII} = 2150$, $\varepsilon_{FeII} = 250$ and $\lambda' = 365$ nm, $\Phi = 1.21$, $\varepsilon_{FeIII} = 700$ and $\varepsilon_{FeII} = 75$. Units of ε are L mol^{-1} cm^{-1}. The sampling time was chosen to deliver at least 20 points over the curved portion of each plot. For each run, absorbances at two wavelengths (one being the irradiation wavelength) were recorded simultaneously. Pure toluene or water was used as reference. All the experimental parameters were assumed to be accurate at ±5%.

5.2. Data treatment

The data were transferred and stored on a HP9000/380 workstation. Simulation and optimisation procedures were performed by using numerical integration [35] and a non-linear minimisation algorithm for the fitting of the model to the experimental data.

Kinetic rate and related algebraic equations for the photochromic process shown in Scheme 2 are

$$\frac{d[A]}{dt} = -\Phi_{AB}^{\lambda'} I_0^{\lambda'} \varepsilon_A^{\lambda'} F[A] + (\Phi_{BA}^{\lambda'} I_0^{\lambda'} \varepsilon_B^{\lambda'} F + k_{BA})[B]$$

with $F = (1 - 10^{-Abs'})/Abs'$ (photokinetic factor), λ' referring to the irradiation wavelength and

$$[B] = [A]_0 - [A]; \; Abs^{\lambda} = \varepsilon_A^{\lambda}[A] + \varepsilon_B^{\lambda}[B] \qquad (1 = 1\,cm)$$

where λ refers to any observation wavelength.

The kinetic rate and related equations for the photodegradation process shown in Scheme 3 are

$$\frac{d[A]}{dt} = -(\Phi_{AB}^{\lambda'} + \Phi_{AE}^{\lambda'}) I_0^{\lambda'} \varepsilon_A^{\lambda'} F[A] + (\Phi_{BA}^{\lambda'} I_0^{\lambda'} \varepsilon_B^{\lambda'} F + k_{BA})[B]$$

$$\frac{d[B]}{dt} = \Phi_{AB}^{\lambda'} I_0^{\lambda'} \varepsilon_A^{\lambda'} F[A] - (\Phi_{BA}^{\lambda'} I_0^{\lambda'} \varepsilon_B^{\lambda'} F + k_{BA} + k_{BC})[B]$$

$$[C] + [E] = [A]_0 - [A] - [B];$$

$$Abs^{\lambda} = \varepsilon_A^{\lambda}[A] + \varepsilon_B^{\lambda}[B] + \varepsilon_C^{\lambda}([C] + [E]) \qquad (1 = 1\,cm)$$

Spectral calculations were performed by application of the Beer–Lambert's law and using the values of concentrations calculated from the model.

References

[1] Organic Photochromic and Thermochromic Compounds, in: J. Crano, R. Guglielmetti (Eds.), vol. 1 and 2, Plenum Publishing Corporation, New York, USA, 1998.
[2] S. Aramaki, G.H. Atkinson, Chem. Phys. Lett. 170 (1990) 181.
[3] N. Tamai, H. Masuhara, Chem. Phys. Lett. 191 (1992) 189.
[4] F. Wilkinson, D.R. Worrall, J. Hobley, L. Jansen, S.L. Williams, A.J. Langley, P. Matousek, J. Chem. Soc., Faraday Trans. 92 (1996) 1331.
[5] J. Aubard, New trends in Raman studies in organic photochroms, in: J. Crano, R. Guglielmetti (Eds.), Organic Photochromic and Thermochromic Compounds, vol. 2, Plenum Publishing Corporation, New York, USA, pp. 349–384.
[6] C. Bohne, M.G. Fan, Z.J. Li, J. Lusztyk, J.C. Scaiano, J. Chem. Soc., Chem. Commun. (1990) 571.
[7] C. Bohne, M.G. Fan, Z.J. Li, Y.C. Liang, J. Lusztyk, J.C. Scaiano, J. Photochem. Photobiol. A: Chem. 66 (1992) 79.
[8] A. Kellmann, F. Tfibel, R. Guglielmetti, J. Photochem. Photobiol. A: Chem. 91 (1995) 131.
[9] E. Pottier, R. Dubest, R. Guglielmetti, P. Tardieu, A. Kellmann, F. Tfibel, P. Levoir, J. Aubard, Helv. Chim. Acta 73 (1990) 303.
[10] G. Favaro, F. Masetti, U. Mazucatto, G. Ottavi, P. Allegrini, V. Malatesta, J. Chem. Soc., Faraday Trans. 90 (1994) 333.
[11] G. Baillet, R. Guglielmetti, G. Giusti, Mol. Cryst. Liq. Cryst. 246 (1994) 287.
[12] G. Favaro, V. Malatesta, U. Mazucatto, C. Miliani, G. Ottavi, Proc. Ind. Acad. Sci. (Chem. Sci.) 107 (1995) 659.
[13] C. Salémi-Delvaux, B. Luccioni-Houzé, G. Baillet, G. Giusti, R. Guglielmetti, J. Photochem. Photobiol. A: Chem. 91 (1995) 223.
[14] G. Baillet, V. Lokshine, R. Guglielmetti, G. Giusti, C.R. Acad. Sci. 319 (1994) 41.
[15] V. Malatesta, M. Milosa, R. Millini, L. Lanzani, P. Bortolus, S. Monti, Mol. Cryst. Liq. Cryst. 246 (1994) 303.
[16] V. Malatesta, F. Renzi, M.L. Wis, L. Montanari, M. Milosa, D. Scotti, J. Org. Chem. 60 (1995) 5446.
[17] C. Salémi, G. Giusti, R. Guglielmetti, J. Photochem. Photobiol. A: Chem. 86 (1995) 247.
[18] V. Malatesta, Mol. Cryst. Liq. Cryst. 298 (1997) 69.
[19] D. Eloy, C. Gay, P. Jardon, J. Chim. Phys. 94 (1997) 683.
[20] H. Rau, G. Greiner, G. Gauglitz, H. Meir, J. Phys. Chem. 94 (1990) 6523.
[21] Y.A. Malkin, T.B. Krasieva, V.A. Kuzmin, Izv. Akad. Nauk. SSSR, Ser. Khim (Engl. Ed.) 2 (1990) 236.
[22] V. Pimienta, D. Lavabre, G. Levy, A. Samat, R. Guglielmetti, J.C. Micheau, J. Phys. Chem. 100 (1996) 4485.
[23] M.H. Deniel, J. Tixier, B. Luccioni-Houzé, D. Lavabre, J.C. Micheau, Mol. Cryst. Liq. Cryst. 298 (1997) 121.
[24] M.H. Deniel, D. Lavabre, J.C. Micheau, Photokinetics under continuous irradiation, in: J. Crano, R. Guglielmetti (Eds.), Organic

Photochromic and Thermochromic Compounds, vol. 2, Plenum Publishing Corporation, New York, 1998, pp. 159–201.
[25] G. Favaro, V. Malatesta, U. Mazzucato, G. Ottavi, A. Romani, Mol. Cryst. Liq. Cryst. 246 (1994) 299.
[26] A.S. Kholmanskii, K.M. Dumayev, Dokl. Akad. Nauk SSSR 303 (1988) 1189.
[27] A.A. Firth, D.J. LMcGarvey, T.G. Truscott, Mol. Cryst. Liq. Cryst. 246 (1994) 295.
[28] V. Malatesta, C. Neri, M.L. Wis, L. Montanari, R. Millini, J. Am. Chem. Soc. 119 (1997) 3451.
[29] F. Wilkinson, J. Hobley, M. Naftaly, J. Chem. Soc., Faraday Trans. 88 (1992) 1511.
[30] G. Favaro, V. Malatesta, U. Mazzucato, G. Ottavi, A. Romani, J. Photochem. Photobiol. A: Chem. 87 (1995) 235.
[31] N.Y.C. Chu, Can. J. Chem. 98 (1983) 300.
[32] D. Eloy, P. Escaffre, R. Gautron, P. Jardon, J. Chim. Phys. 89 (1992) 897.
[33] G. Baillet, M. Campredon, R. Guglielmetti, G. Giusti, C. Aubert, J. Photochem. Photobiol. A: Chem. 83 (1994) 147.
[34] A.M. Braun, M.T. Maurette, E. Oliveros, Photochemical Technology, Wiley, 1991.
[35] K. Kaps, P. Rentrop, Comput. Chem. Eng. 8 (1984) 393 and references cited therein.